

Recent trends in summer atmospheric circulation in the North Atlantic/European region: is there a role for anthropogenic aerosols?

Article

Published Version

Creative Commons: Attribution 4.0 (CC-BY)

Open Access

Dong, B. ORCID: <https://orcid.org/0000-0003-0809-7911> and Sutton, R. T. ORCID: <https://orcid.org/0000-0001-8345-8583> (2021) Recent trends in summer atmospheric circulation in the North Atlantic/European region: is there a role for anthropogenic aerosols? *Journal Of Climate*, 34 (16). pp. 6777-6795. ISSN 1520-0442 doi: <https://doi.org/10.1175/JCLI-D-20-0665.1> Available at <https://centaur.reading.ac.uk/98580/>

It is advisable to refer to the publisher's version if you intend to cite from the work. See [Guidance on citing](#).

To link to this article DOI: <http://dx.doi.org/10.1175/JCLI-D-20-0665.1>

Publisher: American Meteorological Society

All outputs in CentAUR are protected by Intellectual Property Rights law, including copyright law. Copyright and IPR is retained by the creators or other copyright holders. Terms and conditions for use of this material are defined in the [End User Agreement](#).

www.reading.ac.uk/centaur

CentAUR

Central Archive at the University of Reading

Reading's research outputs online

Recent Trends in Summer Atmospheric Circulation in the North Atlantic/European Region: Is There a Role for Anthropogenic Aerosols?

BUWEN DONG^a AND ROWAN T. SUTTON^a

^a*National Centre for Atmospheric Science, Department of Meteorology, University of Reading, Reading, United Kingdom*

(Manuscript received 21 August 2020, in final form 20 May 2021)

ABSTRACT: The variability of the westerly jet stream and storm track is crucial for summer weather and climate in the North Atlantic/European region. Observations for recent decades show notable trends in the summer jet from the 1970s to 2010s, characterized by an equatorward migration over the North Atlantic accompanied by a poleward migration and weakening of the Mediterranean jet over Europe. These changes in atmospheric circulation were associated with more cyclonic storms traveling across the United Kingdom into northern Europe, and fewer over the Mediterranean, leading to wet summers in northern Europe and dry summers in southern Europe. In this study we investigate the potential drivers and processes that may have been responsible for the observed changes in summer atmospheric circulation, with a particular focus on the role of anthropogenic aerosols (AA). We conduct attribution experiments with an atmospheric general circulation model (AGCM) forced with observed changes in sea surface temperatures/sea ice extent (SST/SIE), greenhouse gas concentrations, and AA precursor emissions. Comparison between the model results and observations strongly suggests that fast responses to AA changes were likely the primary driver of the observed poleward migration and weakening of the Mediterranean jet, with changes in SST/SIE playing a secondary role. The simulated response shows good agreement with the observed changes in both magnitude and vertical structure, which suggests that common mechanisms, involving aerosol–radiation and aerosol–cloud interactions, are responsible. By contrast, changes in the North Atlantic jet are influenced in the model experiments by changes in both Atlantic SST/SIE (which may themselves have been influenced by changes in AA) and fast responses to AA. In this case, however, there are significant differences between the model response and the observed changes; we argue that these differences may be explained by biases in the model climatology.

KEYWORDS: Atmospheric circulation; Decadal variability; Jets; Storm tracks


1. Introduction


Atmospheric circulation in the North Atlantic region exhibits variability on a wide range of time scales, and exerts a major influence on the geographical distribution of precipitation and temperature over the North Atlantic Ocean and surrounding continents in both winter and summer. Much of this variability is associated with fluctuations in the westerly jet stream and storm track, such as those associated with the North Atlantic Oscillation (NAO) (e.g., Hurrell et al. 2003; Dong et al. 2013a,b; Iles and Hegerl 2017; Robson et al. 2018; Simpson et al. 2018).

Recent studies have shown that year-to-year fluctuations in the atmospheric circulation in summer can lead to extreme climate conditions over Europe (Baldi et al. 2006; Blackburn et al. 2008; Dong et al. 2013a,b; Ossó et al. 2018). For example, summer 2007 in the United Kingdom was very wet, with record rainfall and flooding associated with a distinctive westerly jet

pattern (Blackburn et al. 2008). Summer 2012—when the United Kingdom experienced its wettest summer for a century and Spain experienced low rainfall and drought—was characterized by a southward displacement of the eddy-driven jet (Dong et al. 2013a). Another important branch of summer circulation over the North Atlantic sector that affects summer climate over Europe is the Mediterranean jet, governed by the thermal contrast between the African warm air and the European cool air (Baldi et al. 2006). Baldi et al. (2006) showed that interannual variability of summer climate in the Mediterranean was associated with different configurations of the North Atlantic eddy driven-jet and the subtropical Mediterranean jet. Hot summers in the Mediterranean were related to a more zonally elongated eddy-driven jet, corresponding to a southward displacement of the westerly jet at the Atlantic jet exit region and a northward displacement at the entrance region of the subtropical Mediterranean jet whereas cool summers were associated with opposite changes in these two jets.

Significantly, while individual extreme years stand out in historical records, these same records show notable trends on decadal time scales. In particular, since the 1980s, there was a prominent equatorward (i.e., southward) migration of the

 Denotes content that is immediately available upon publication as open access.

 Supplemental information related to this paper is available at the Journals Online website: <https://doi.org/10.1175/JCLI-D-20-0665.s1>.

Corresponding author: Buwen Dong, b.dong@reading.ac.uk

DOI: 10.1175/JCLI-D-20-0665.1



This article is licensed under a [Creative Commons Attribution 4.0 license](http://creativecommons.org/licenses/by/4.0/) (<http://creativecommons.org/licenses/by/4.0/>).

North Atlantic eddy-driven jet (Fig. 2 of [Robson et al. 2018](#)), associated with increased Greenland blocking and a negative trend in the summer North Atlantic Oscillation (NAO) index ([Hanna et al. 2015, 2018](#)). These changes in atmospheric circulation favored cooler and wetter summers in northwestern Europe, suggesting that the trends may have contributed to increasing the risk of extreme wet summers, such as those that occurred in 2007 and 2012. It follows that understanding the mechanisms that shape variability and trends in the North Atlantic summer circulation is an important challenge for understanding the risk of high impact weather and climate events and hence for mitigating the societal, economic, and ecological impacts that arise from such events.

There are a number of suggested influences on the low-frequency variation of the North Atlantic summer jet stream and SNAO (e.g., [Folland et al. 2009](#); [Dong et al. 2013a,b](#); [Hall et al. 2015, 2017](#); [Osborne et al. 2020](#)). One such influence is low-frequency variations in Atlantic sea surface temperatures associated with the Atlantic multidecadal variability (AMV). The AMV positive phase, characterized by an anomalously warm North Atlantic Ocean, is associated with a southward shift of the eddy-driven jet, a negative SNAO, and wet summers in northwestern Europe ([Knight et al. 2006](#); [Folland et al. 2009](#); [Sutton and Hodson 2005, 2007](#); [Sutton and Dong 2012](#); [Ghosh et al. 2017](#); [O'Reilly et al. 2017](#)).

Anthropogenic aerosols affect global and regional climate through aerosol–radiation and aerosol–cloud interactions (e.g., [Boucher et al. 2013](#)). Because of their inhomogeneous spatial distributions, aerosols can cause changes in horizontal and vertical temperature gradients, which in turn affect atmospheric circulation ([Rotstajn et al. 2013](#); [Shen and Ming 2018](#); [Undorf et al. 2018a](#)), potentially including the strength and position of the Northern Hemisphere subtropical jet stream ([Undorf et al. 2018a](#)). Anthropogenic aerosols may affect atmospheric circulation directly through a fast response of the atmosphere and land surface and also more slowly through aerosol-induced changes in sea surface temperatures (SSTs), such as a potential influence on AMV ([Booth et al. 2012](#); [Undorf et al. 2018a,b](#); [Watanabe and Tatebe 2019](#)). However, in contrast to their thermodynamic effects on temperatures, a detailed understanding of how changes in anthropogenic aerosol forcing may have affected atmospheric circulation in the North Atlantic region is still lacking.

The aim of this study is to explore further recent decadal changes in the summertime atmospheric circulation in the North Atlantic/European region and to investigate the drivers and mechanisms by performing numerical experiments with an atmospheric general circulation model. A specific focus is investigating changes in the North Atlantic and Mediterranean jet streams and the potential role of the fast response to changes in anthropogenic aerosols. Our approach to regional attribution, which seeks to identify the influence of specific drivers on particular observed changes, is in line with the storyline perspective advocated by [Shepherd \(2019\)](#) to understand regional climate change.

2. Observational datasets and recent decadal trends

a. Observational datasets and analysis methods

The observational datasets used for the analyses in this study are the NCEP–NCAR reanalysis data ([Kalnay et al. 1996](#)), the Met Office Hadley Centre mean sea level pressure (SLP) data HadSLP2 ([Allan and Ansell 2006](#)), the monthly CRU TS4.03 precipitation and surface temperature datasets ([Harris et al. 2014](#)), and the monthly mean SST dataset of HadISST ([Rayner et al. 2003](#)).

Following [Woollings et al. \(2014\)](#), jet latitude is defined as the location of the maximum westerly wind speed zonally averaged over a sector at 500 hPa using seasonal mean data. Storm track analysis is based on the tracking scheme developed by [Hodges \(1994\)](#). Cyclones are identified as 850-hPa relative vorticity maxima at 6-hourly frequency using the NCEP reanalysis. Blocking frequency is based on the index introduced by [Tibaldi and Molteni \(1990\)](#) and extended to two dimensions by [Scherrer et al. \(2006\)](#) using NCEP daily mean geopotential height at 500 hPa. The AMV index is defined as area averaged SST over the region (0° – 60° N, 75° – 7.5° W) with an 11-yr running mean.

b. Recent decadal trends in observations and their impacts on European climate

Illustrated in [Fig. 1](#) are the first empirical orthogonal functions (EOF1) of zonal wind at 500 hPa ([Fig. 1a](#)) and storm track density ([Fig. 1c](#)) over the North Atlantic/European sector for June, July, and August (JJA) with the corresponding principal components (PC1) in [Figs. 1b and 1d](#). The dominant mode of zonal wind (storm track) variability is characterized by a dipole structure with positive anomalies to the north of the climatological jet (maximum track density) and negative anomalies to the south during the positive phase. This corresponds to a northward displacement of the eddy-driven jet and storm track during their positive phases. This mode is also associated with some changes in the Mediterranean jet with the positive phase being associated with an enhanced and southward displaced jet and increased storm activity over the Mediterranean Sea ([Figs. 1a,c](#)). The time variations of the zonal wind mode and storm track mode are very highly correlated with a correlation coefficient of 0.90 (0.96 for low-frequency variations). The time variations of the zonal wind mode are also highly correlated with the variability of the North Atlantic jet latitude with a correlation coefficient of 0.77 (0.90 for low-frequency variations) ([Fig. 1b](#)).

All the various indices exhibit low-frequency decadal variability in addition to interannual fluctuations. Particularly prominent is the southward trend in jet latitude and storm track density over the North Atlantic from the 1970s to the 2010s. Accompanying this southward trend are trends in blocking frequency, with increases over Greenland, and decreases over western Europe ([Fig. 1d](#) herein and [Fig. S1](#) in the online supplemental material; see also [Hanna et al. 2018](#)). [Figures 1e and 1f](#) compare selected circulation indices with indices of surface temperature (see caption for details). [Figure 1e](#) shows that decadal variations in the latitude of the Mediterranean jet are highly correlated with an index of the

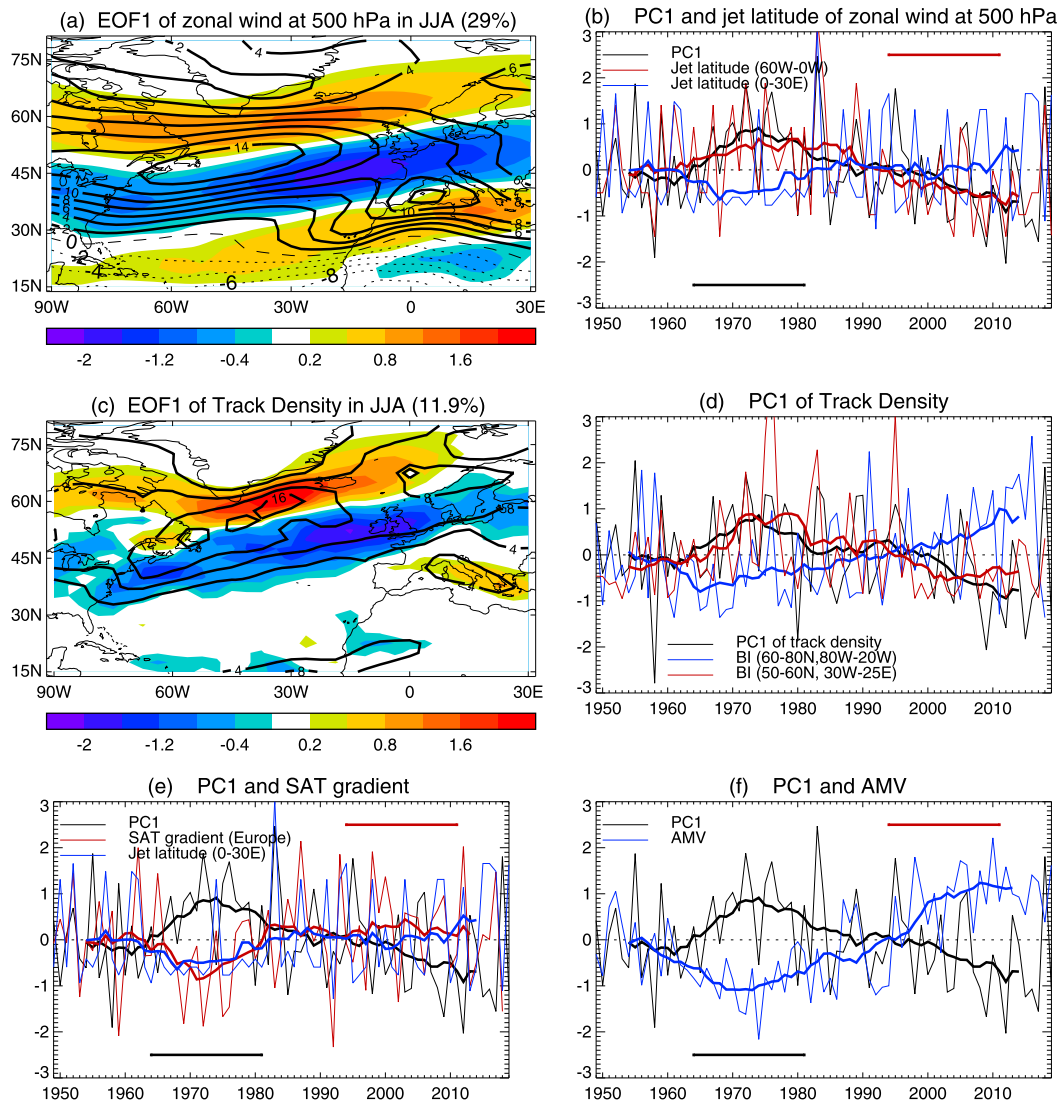


FIG. 1. EOF1 (colors) of (a) zonal wind (m s^{-1}) at 500 hPa and (c) storm track density interannual variability in JJA for period 1949–2019 with the climatology of 1964–2011 (contours) based on observations (reanalysis). (b) The corresponding PC1 for zonal wind at 500 hPa and normalized time series of the jet latitude at sectors of 60° – 0° W and 0° – 30° E. Black and red bars highlight two periods of 1964–81 and 1994–2011. (d) PC1 of storm track variability and blocking indices over Greenland (60° – 80° N, 80° – 20° W) and western Europe (50° – 60° N, 30° – 0° W). Blocking frequency is based on the index introduced by Tibaldi and Molteni (1990) and extended to two dimensions by Scherrer et al. (2006). (e) PC1 of zonal wind at 500 hPa, the meridional SAT gradient over western European sector over land between the southern region (30° – 45° N, 0° – 30° E) and the northern region (45° – 65° N, 0° – 30° E) (boxes in Fig. 3b) for 1949–2018, and the jet latitude at sector of 0° – 30° E. (f) PC1 of zonal wind at 500 hPa and the Atlantic multidecadal variability (AMV) index, defined as area-averaged SST over the region 0° – 60° N, 75° – 7.5° W. Thick lines in (b), (d), (e), and (f) are 11-yr running means. Storm track densities are in units of number density per month per unit area, where the unit area is equivalent to a 5° spherical cap ($\sim 10^6 \text{ km}^2$). Zonal wind and storm track densities are based on the NCEP reanalysis.

meridional surface air temperature (SAT) gradient between southern Europe and northern Europe, and anticorrelated with PC1 of the zonal wind. It shows that from the 1970s to 2010s there was a southward displacement of the North Atlantic jet associated with an enhanced meridional SAT gradient over western Europe and a northward

displacement of the Mediterranean jet. Figure 1f compares PC1 of the zonal wind with the AMV index, and confirms the negative correlation between these indices (e.g., Knight et al. 2006; Folland et al. 2009; Sutton and Hodson 2005, 2007; Sutton and Dong 2012; Ghosh et al. 2017). In particular, the southward displacement of the North Atlantic jet

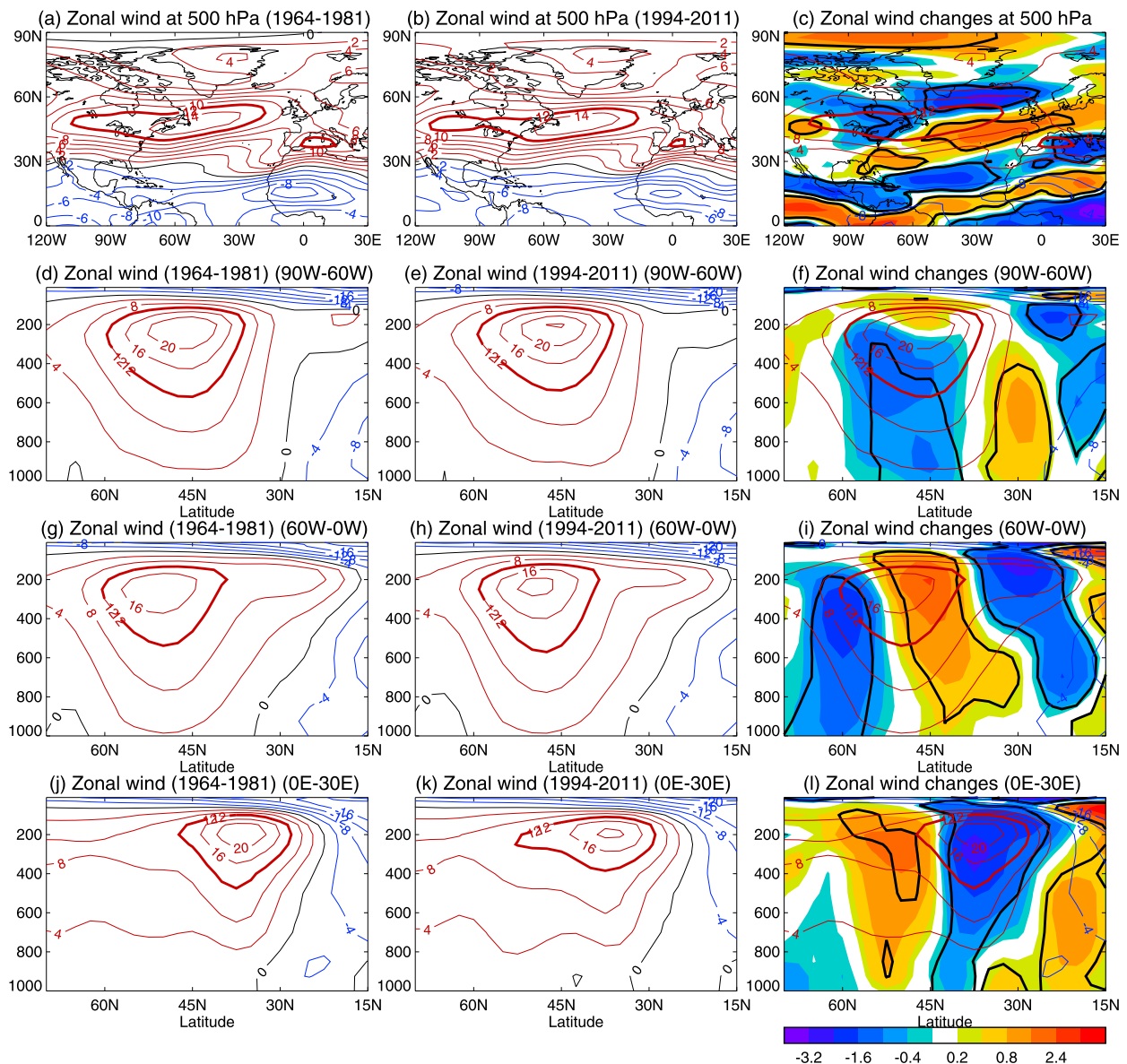


FIG. 2. Decadal mean zonal winds and changes (m s^{-1}) between 1994–2011 and 1964–81 in JJA based on the NCEP reanalysis. (left) Zonal wind for the period 1964–81, (center) zonal wind for 1994–2011, and (right) changes (color) between 1994–2011 and 1964–81, with 1964–81 zonal winds plotted in contours. (a)–(c) Zonal wind at 500 hPa. (d)–(l) Zonal wind at the sectors 90° – 60° W, 60° – 0° W, and 0° – 30° E. Thick black lines in (c), (f), (i), and (l) highlight regions where changes are statistically significant at 10% level based on the two-tailed Student's t test.

since the 1970s is associated with a positive trend in the AMV index.

To investigate these changes in greater detail we examine differences between means over two time periods: 1964–81 and 1994–2011. We chose these two periods to avoid major volcanic eruptions but still capture significant trends in the various indices shown in Fig. 1. Figure 2 shows zonal winds at 500 hPa, and zonally averaged zonal winds for three sectors (i.e., longitude bands) for each of the two time periods and for the corresponding changes between two periods. Compared with

1964–81, zonal winds at 500 hPa in 1994–2011 were more zonally elongated at the exit of the North Atlantic jet and the Mediterranean jet was weaker (Figs. 2a,b). Zonal wind changes at 500 hPa between two periods (Fig. 2c) show a similar structure as seen in EOF1 (with a sign change compared to Fig. 1a) with enhanced wind to the south of the climatological jet and weakened wind to the north over the North Atlantic sector (Fig. 2c). However, there are also some interesting differences from EOF1. The zonal wind anomalies in Fig. 2c feature a dipole pattern over eastern North America

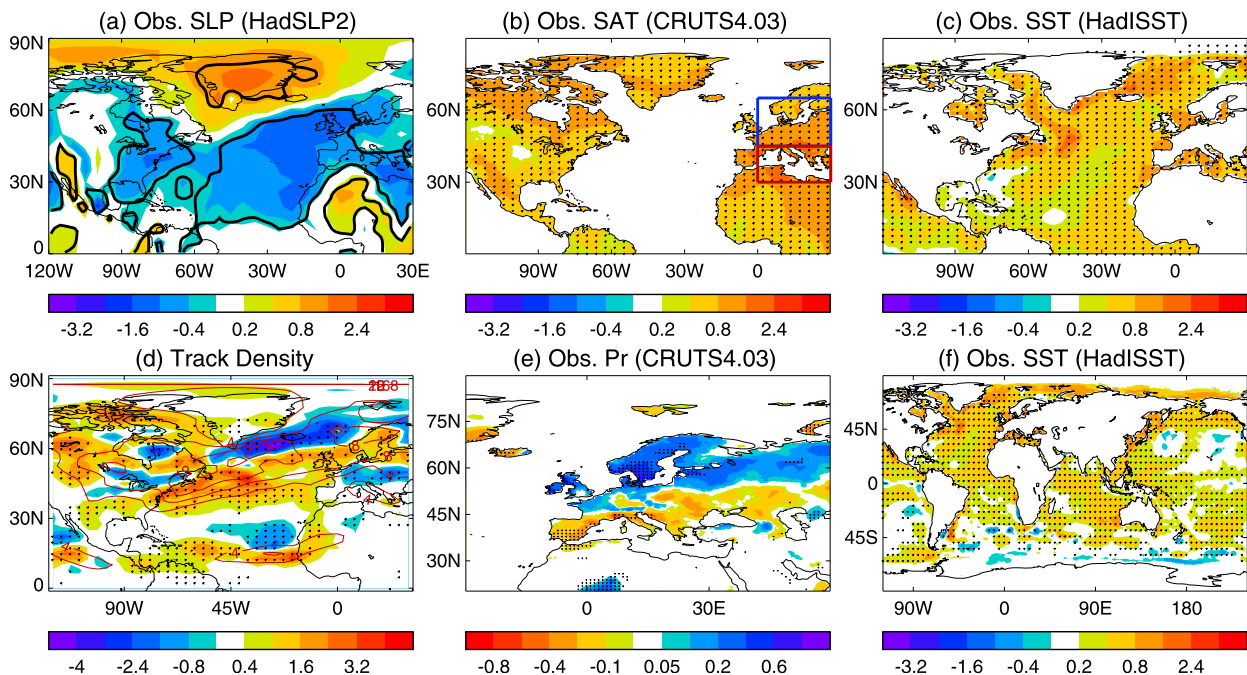


FIG. 3. Decadal changes between 1994–2011 and 1964–81 in JJA based on observations (reanalysis). (a) SLP (hPa) from HadSLP2, (b) surface air temperature ($^{\circ}\text{C}$) from CRU TS4.03, (c) sea surface temperature ($^{\circ}\text{C}$) over the North Atlantic from HadISST, (d) storm track density based on the NCEP reanalysis, (e) precipitation (mm day^{-1}) from CRUTS4.03, and (f) sea surface temperature ($^{\circ}\text{C}$). Thick lines in (a) and dots in other panels highlight regions where differences are statistically significant at 10% level based on the two-tailed Student's t test. Track densities in (d) are in units of number density per month per unit area, where the unit area is equivalent to a 5° spherical cap ($\sim 10^6 \text{ km}^2$). Boxes in (b) highlight regions that are used for calculating meridional surface air temperature gradient over the western European sector in Fig. 1.

and a separate, much more zonally elongated, dipole pattern over the eastern North Atlantic and western Europe. In Europe, the reduced zonal wind anomalies over the Mediterranean Sea appear separate from similar anomalies over the Atlantic Ocean farther west. This east/west separation is not seen in the EOF pattern (Fig. 1a) and might suggest different drivers for the eastern and western parts of the pattern.

The sectoral cross sections illustrate how the structure of the jet varies across the North Atlantic basin, with the jet maximum located around 45°N over eastern North America, around 50°N over the North Atlantic, and around 35°N over the western European sector (Fig. 2). In the North Atlantic sector zonal winds in the later period, relative to the early period, show a strengthening on the equatorward flank of the jet and weakening on the poleward flank. By contrast, in the western European sector the jet weakened, and also broadened on its poleward flank. The vertical structure of the zonal wind changes in each sector is substantially equivalent barotropic, with the largest anomalies in the North Atlantic and western European sectors located in the upper troposphere. The field significance of zonal wind changes at 500 hPa for the region and for three sectors between two periods is established using a bootstrap method (e.g., Livezey and Chen 1983). The bootstrap sampling is conducted 1000 times by randomly selecting two 18-yr chunks from the period 1964–2011.

The statistic fraction of grids with significant changes is used to construct a probability distribution. The fractions of grids that show significant changes between two periods at 500 hPa and for the three sectors are 0.40, 0.27, 0.48, and 0.41. These fractions lie above the 90th percentiles of bootstrap samples that are 0.20, 0.23, 0.24, and 0.25, respectively, suggesting that the zonal wind changes between the two periods are very unlikely to be due to sampling uncertainty. In Fig. S2d these wind changes are decomposed into baroclinic and residual barotropic components. In general but not everywhere the baroclinic component is larger. The residual barotropic components are consistent with changes in meridional SLP gradients (Figs. S2j–l and Fig. 3a).

Figure 3 illustrates the changes between two periods in several other important variables. Associated with the southward displacement of the North Atlantic eddy-driven jet are negative SLP anomalies over the North Atlantic and western Europe, and positive SLP anomalies over Greenland (Fig. 3a). This pattern projects on the negative phase of the summer NAO (e.g., Folland et al. 2009; Dong et al. 2013a,b) and is associated with a southward displacement of the storm track (Fig. 3d) and with enhanced blocking over Greenland and reduced blocking over western Europe (Fig. S1). Storm activity across the United Kingdom into northwestern Europe increased, whereas storm activity over southern Europe decreased. Associated with these anomalies in storminess was

TABLE 1. Summary of numerical experiments using MetUM-GA6 for recent decadal changes.

Experiments	Boundary conditions
CON	Monthly climatological sea surface temperature (SST) and sea ice extent (SIE) averaged over the period of 1964–81 using HadISST (Rayner et al. 2003) with greenhouse gas (GHG) concentrations over the same period, and anthropogenic aerosol (AA) precursor emissions (Lamarque et al. 2010) at mean values over the period 1970–81
ALL	Monthly climatological SST/SIE averaged over the period of 1994–2011, with GHGs and AA emissions (Lamarque et al. 2011) over 1994–2011
SSTAA	SST/SIE as in ALL, AA as in ALL, GHGs as in CON
SST	SST/SIE as in ALL, AA as in CON, GHGs as in CON
SSTNoAtl	SST/SIE over the Atlantic Ocean (northward of 30°S over the Atlantic but excluding the Mediterranean Sea) as in CON, SST/SIE elsewhere as in ALL, AA as in CON, GHGs as in CON

increased precipitation over northern Europe and reduced precipitation over southern Europe in the more recent period of 1994–2011 relative to the early period of 1964–81 (Figs. 3d,e).

Also illustrated in Fig. 3 are changes in surface temperatures between the two periods. Sea surface temperatures warmed in many regions but particularly in the mid-high latitude North Atlantic associated with the transition to the positive phase of AMV (Figs. 3c,f). Surface air temperatures also warmed over North America and Europe with the strongest warming seen in the Mediterranean region (Fig. 3b).

Figures 1–3 demonstrate that substantial changes in atmospheric circulation occurred in the North Atlantic region between 1964–81 and 1994–2011. Note that the changes in observations between the two periods are not purely due to changes in external forcing, such as greenhouse gases (GHGs), anthropogenic aerosol (AA) concentrations, or natural forcing associated with volcanic eruptions and solar variability: they are a combination of external forced changes and internally driven atmospheric variability (e.g., Deser and Phillips 2009; Simpson et al. 2018). However, we now seek to investigate what forcing factors may have contributed to these changes, and to understand the physical processes involved.

3. Atmospheric model experiments

a. Model and experiments

The model used is the latest Met Office atmosphere and land model GA6.0 (MetUM-GA6; see Walters et al. 2017) with a resolution of 1.875° longitude \times 1.25° latitude and 85 levels in the vertical. The model includes a prognostic tropospheric aerosol model using the CLASSIC (Coupled Large-scale Aerosol Simulator for Studies in Climate) aerosol scheme and eight aerosol species (ammonium sulfate, mineral dust, fossil-fuel black carbon, fossil-fuel organic carbon, biomass-burning, ammonium nitrate, sea-salt, and secondary organic aerosols from biogenic emissions). Both aerosol–radiation and aerosol–cloud interactions are considered (Bellouin et al. 2011).

Relative to the baseline period of 1964–81, there were changes in several potential drivers of regional climate in the later period of 1994–2011. Sea surface temperatures warmed, with large warming anomalies over the North Atlantic sub-polar gyre (Fig. 3c) and over the tropical Indian Ocean and

western Pacific (Fig. 3f). There were associated changes in sea ice extent (SIE), particularly in the Arctic (not shown). Greenhouse gas (GHG) concentrations also increased (14% increase in CO₂, 23% increase in CH₄, and 7% increase in N₂O), and there were significant changes in anthropogenic aerosol (AA) emissions. The changes in annual mean sulfur dioxide emissions, the major aerosol precursor emissions, involve decreases over Europe and North America and increases over East and South Asia [see Fig. 1 of Undorf et al. (2018a) and Fig. 3 of Chen and Dong (2019)]. A set of experiments (62 years long each) was carried out to identify the roles of changes in 1) global SST/SIE, 2) Atlantic SST/SIE, confined to the region northward of 30°S and bounded by the Americas to the west and Africa and Europe to the east, 3) anthropogenic GHGs, and 4) AA forcings (precursor emissions of all species) in shaping the changes of the summer mean circulation over the North Atlantic/European sector. Note that the impacts of changes in GHGs and AA in these experiments refer to fast responses of the atmosphere and land surface to the forcing changes and do not include slower changes mediated through induced SST changes. The experiments are as follows: CON forced by the early period (1964–81) SST/SIE climatology, GHGs, and appropriate AA; ALL forced by the recent period (1994–2011) SST/SIE, GHGs, and AA; SSTAA forced by the recent period SST/SIE and AA with the early period GHGs; SST forced by the recent period SST/SIE with the early period GHGs and AA; and SSTNoAtl forced by the recent period SST/SIE outside Atlantic Ocean (including the Mediterranean Sea) with the early period GHGs and AA. Further details of the experiments are documented in Table 1. This experimental design to assess responses to different forcing factors assumes that these responses are additive (see later discussion). Note that a slightly different period for the aerosol forcing is used in CON experiment since aerosol emissions data before 1970 were not available locally when the experiments were set up. We have checked aerosol emission data and the differences between means of 1970–81 and those of 1964–81 are small (not shown) and therefore it is expected that the resultant climatic effect is weak. In this set of experiments, SST/SIE is taken as an independent forcing factor and responses to changes in GHGs and AA only consider the fast atmospheric and land responses. The last 60 years of each experiment are analyzed and the response to a particular forcing is estimated by the difference between a pair of experiments that include and exclude that

particular forcing. The impact of changes in Atlantic SST/SIE is estimated from the difference between experiment SST and experiment SSTNoAtl. Statistical significance of the summer mean changes is assessed using a two-tailed Student's *t* test.

b. Model climatology and biases in the North Atlantic region

It is important to evaluate the model climatology as biases can potentially affect the simulated circulation response to external forcing (e.g., Baker et al. 2017, 2019; Osborne et al. 2020). Figure 4 shows the simulated zonal winds at 500 hPa and zonally averaged zonal winds for three sectors for the early period (1964–81) in the CON experiment, together with model biases relative to the NCEP reanalysis. Zonal wind biases at 500 hPa show distinct dipole patterns over the North American, North Atlantic, and western European sectors with statistically significant positive anomalies to the north of the jet axis and negative anomalies to the south and indicate that the model-simulated jet is biased northward by about 2° – 3° in latitude, similar to biases seen in CMIP5 models (e.g., Iqbal et al. 2018). The North Atlantic jet extends too far eastward over Europe and is less well separated from the Mediterranean jet in the model than in the reanalysis. The simulated Mediterranean jet at 500 hPa is about 2 m s^{-1} weaker than in the reanalysis.

Vertical cross sections of the zonal wind biases provide further information (Figs. 4d,f,h). Over the North American sector, the main feature is a significant negative bias over a broad latitude range of 30° – 50°N with a fairly barotropic structure (Figs. 4c,d). Over the North Atlantic sector, the northward bias in the jet latitude is highlighted by a dipole pattern of westerly anomalies, with the largest significant anomalies located in the upper troposphere (Figs. 4e,f). Over Europe, it can be seen that the Mediterranean jet in the model is too weak, particularly on the equatorward side, and somewhat too broad (Figs. 4g,h). The largest anomalies are again located in the upper troposphere, although the vertical structure is substantially equivalent barotropic.

To address whether the model biases in zonal winds are sensitive to sampling uncertainty, we also analyzed model biases during the period of 1994–2011 and biases for the combined two 18-yr periods. These are illustrated in Figs. S3 and S4. As shown by these figures, the spatial patterns and magnitudes of biases are very similar to those shown in Fig. 4, indicating these biases are robust and unlikely to have been strongly influenced by sampling uncertainty. The zonal wind biases in summer are also not very sensitive to model horizontal resolution (not shown). Investigating the causes of these biases is beyond the scope of this paper. However, an awareness of these biases is important for the interpretation of our results.

4. Results: Responses to different forcings

a. Model-simulated circulation changes in response to different forcings

The responses of SLP, 500-hPa zonal wind, and SAT over the North Atlantic/European sector to different forcings are

illustrated in Fig. 5, and may be compared with the observed anomaly patterns (Figs. 3a, 2c, and 3b). In response to changes in ALL forcings together, the model shows weak but significant positive SLP anomalies over North America and northern Europe, and significant negative SLP anomalies over southern Europe and North Africa (Fig. 5a). Accompanying these SLP anomalies are weakened westerlies over North America and western Europe (Fig. 5b). These negative zonal wind anomalies show some agreement with the observed changes (Fig. 3c) but elsewhere—especially over the North Atlantic—the agreement is poor. SAT changes show warming everywhere with relatively large warming over eastern North America, southern Europe, and North Africa (Fig. 5c). In many regions the magnitude of warming is greater than seen in observations (Fig. 3b).

The response to changes in SST/SIE and aerosol emissions together (SSTAA) features a dipole pattern of SLP anomalies with negative anomalies over the subtropics and midlatitudes and positive anomalies at high latitudes over the North Atlantic (Fig. 5d). Interestingly, this pattern of SLP anomalies shows greater similarity to the observed changes (Fig. 3a) than found in the ALL experiment, but relative to observations the pattern of anomalies is shifted southward by about 5° in latitude over the northeast Atlantic and western Europe. Positive SLP anomalies over Greenland extend too far eastward and westward in the model simulations. Associated with the changes in SLP are a weakening and broadening of the westerly jet over the North American and North Atlantic sectors and a dipole pattern of zonal wind anomalies over the western European sector with decreases in zonal winds over the Mediterranean Sea and increases to the north, corresponding to a northward shift of the Mediterranean jet (Fig. 5e). The dipole response over Europe shows improved agreement with the observations compared to the ALL experiment; however, the agreement farther west in the region of the Atlantic jet remains poor. This poor agreement suggests the model may have deficiency in its response to external forcing changes. Alternatively, natural forcing change associated with volcanic eruptions (e.g., Barnes et al. 2016; Undorf et al. 2018b; DallaSanta et al. 2019) and/or internal variability (e.g., Deser and Phillips 2009; Simpson et al. 2018) might have played a significant role in the observed changes.

It is surprising that, in comparison to the response to combined AA and SST/SIE forcings, the response to ALL forcing (not including natural forcing) does not show improved agreement with observations. If the model were perfect and the roles of changes in natural forcing and internal atmospheric variability were weak in the real world, this is not what we would expect. However, the comparison of Fig. 5c with Fig. 3b shows that the model generates too much surface warming over North America and Europe. The implied responses to changes in GHGs are shown in Fig. S5. Note that these implied impacts are inferred from the difference between experiments ALL and SSTAA and they are the responses to GHG changes in the presence of changes in SST/SIE and AA. They show significant positive SLP anomalies in midlatitudes over the North Atlantic and weak negative SLP anomalies over Greenland (Fig. S5a). Accompanying these SLP anomalies is a

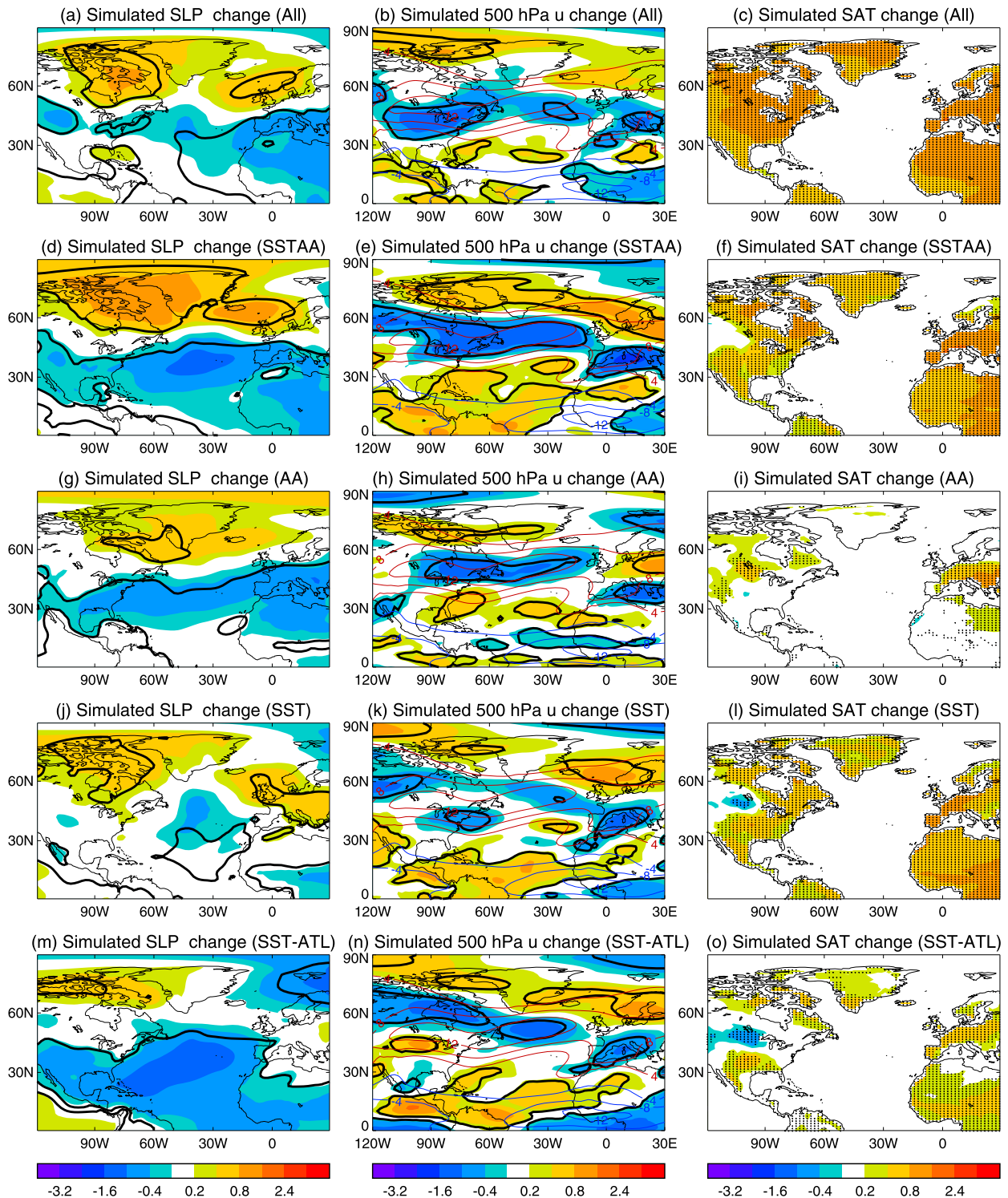


FIG. 5. Simulated climatological seasonal mean responses to different forcings in JJA: (left) SLP (hPa), (center) zonal wind (m s^{-1}) at 500 hPa, and (right) surface air temperature ($^{\circ}\text{C}$). Thin red (westerly) and blue (easterly) lines in middle column are the climatology of the CON simulation (see Table 1 for experiment names and conditions). Thick lines (left and center columns) and dots (right column) highlight regions where differences are statistically significant at 10% level based on the two-tailed Student's t test. (a)–(c) Responses to ALL forcings (ALL – CON), (d)–(f) responses to changes in SST/SIE and AA (SSTAA – CON), (g)–(i) response to changes in AA (SSTAA – SST), (j)–(l) responses to changes in SST/SIE (SST – CON), and (m)–(o) responses to changes in SST/SIE over the Atlantic sector (SST – SSTNoAtl).

northward displacement of the North American jet and an enhancement of the North Atlantic jet (Fig. S5b), features that are opposite to the changes seen in response to combined changes in AA and SST/SIE (Fig. 5). The changes in westerlies over North America are consistent with surface air temperature changes that show large warming over mid North America, associated with increased meridional SAT gradient around 60°N. These changes of westerlies over the North American and North Atlantic sectors are similar to those found in the study of Grise and Polvani (2014), who showed an enhancement of westerlies at 850 hPa (their Fig. 3) over the North American and North Atlantic sectors and weakening of westerlies over the western European sector in response to quadrupled atmospheric CO₂ concentrations. However, changes in GHG concentrations in our experiment are much less than those in the study of Grise and Polvani (2014), which therefore suggests that the impact of GHG forcing on atmospheric circulation in the North Atlantic/European region in our model might be too strong compared to the impact of other forcing factors [assuming the CMIP5 model range studied by Grise and Polvani (2014) is representative of the real world].

Separate forcing simulations indicate that both changes in aerosol emissions and SST/SIE are important factors for the simulated SLP and zonal wind changes over the North American, North Atlantic, and western European sectors (Figs. 5g–l). In particular, changes in aerosol emissions result in a dipole pattern of SLP anomalies with significant positive SLP anomalies over Greenland and negative SLP anomalies over midlatitudes extending from North America across the North Atlantic and into western Europe and North Africa. These SLP anomalies are associated with changes in two regions: 1) over eastern North America and the western Atlantic where the jet weakens and broadens, and 2) over Europe where the dipole pattern of wind anomalies seen in the SSTAA experiment is reproduced (Figs. 5e,h). The AA experiment shows a weak response in the jet over the northeast Atlantic, and in this region the SST/SIE appears to have a stronger influence, contributing to a weakening and northward broadening at the jet exit region (Fig. 5k). A similar change in this region is found in response to changes in Atlantic SST/SIE (Fig. 5n), suggesting that Atlantic SST/SIE anomalies are responsible.

Without GHG changes, the response of SAT is reduced in magnitude, as expected (Figs. 5f,i,l,o). The patterns of SAT response exhibit some interesting features, in particular 1) a local minimum in warming in central North America, which is also seen in observations (Fig. 3b) and appears to be influenced by both AA and SST forcing, and 2) a local maximum in warming in the Mediterranean region, which is also seen in observations and appears to be primarily a response to AA forcing, consistent with other studies (e.g., Ruckstuhl et al. 2008; Nabat et al. 2014; Dong et al. 2017; Tian et al. 2020).

These results suggest that changes in anthropogenic aerosol emissions and changes in sea surface temperatures may have played a significant role in the observed changes in summertime atmospheric circulation in the North Atlantic/European

region. In particular, changes in the Mediterranean jet may have been directly forced by AA changes. AA changes may also have played an important role in shaping changes over eastern North America and the western North Atlantic: for instance, the significant positive SLP anomalies over Greenland seen in the AA experiment suggest that aerosol changes might have been a contributing factor for the recent decadal increase in blocking activity (e.g., Hanna et al. 2015, 2018). To evaluate these hypotheses further, we next investigate the physical processes involved.

b. Physical mechanisms of model simulated changes in atmospheric circulation

1) RESPONSE TO CHANGES IN ANTHROPOGENIC AEROSOLS

In response to recent decadal changes in anthropogenic aerosol emissions, the model simulates a decrease of cloud droplet number concentration (CDNC) by 10%–15%, an increase in cloud droplet effective radius (CDER) by 5%–10%, and a decrease in aerosol optical depth with large decreases over North America, across the North Atlantic, and over western Europe (Figs. 6a–c) due to decreased emissions over North America and Europe. These changes result in large positive anomalies in surface clear-sky shortwave radiation through aerosol–radiation interactions with local maxima about 4–6 W m^{−2} over North America and about 8–10 W m^{−2} over western Europe. All-sky surface shortwave radiation shows similar patterns, but with additional features arising from changes in clouds (Figs. 6d,e,g,h). Decreases in cloud fraction over North America and Europe are partly due to decrease in AA emissions through aerosol–cloud interactions (e.g., Boucher et al. 2013) and partly due to decrease in relative humidity in the lower troposphere (Fig. 6f). The reduced relative humidity is the result of reduced evaporation and that specific humidity over land regions increases less than specific humidity at saturation (e.g., Boé and Terray 2014; Dong et al. 2017). These changes in surface shortwave radiation lead to an inhomogeneous surface warming over North America and Europe, characterized by enhanced warming over North America and southern Europe (Fig. 6i).

Figure 7 illustrates the vertical structure of zonally averaged zonal wind responses to AA emissions over the three sectors. The zonal wind response in each sector is partitioned into a baroclinic component, related to meridional temperature gradients and a residual barotropic component. Over the European sector, the baroclinic component dominates. Anomalies in meridional temperature gradients peak near the surface and are characterized by decreases at 30°–45°N and increases at 45°–60°N (Fig. 7f), consistent with changes in SAT gradients (Fig. 6i). These findings suggest that *the poleward shift in the Mediterranean jet in response to AA changes is caused by anomalous surface temperature gradients induced by changes in surface shortwave radiation.*

Over the North American sector, the baroclinic component again dominates, although the barotropic component has larger magnitude than in the European sector. There is

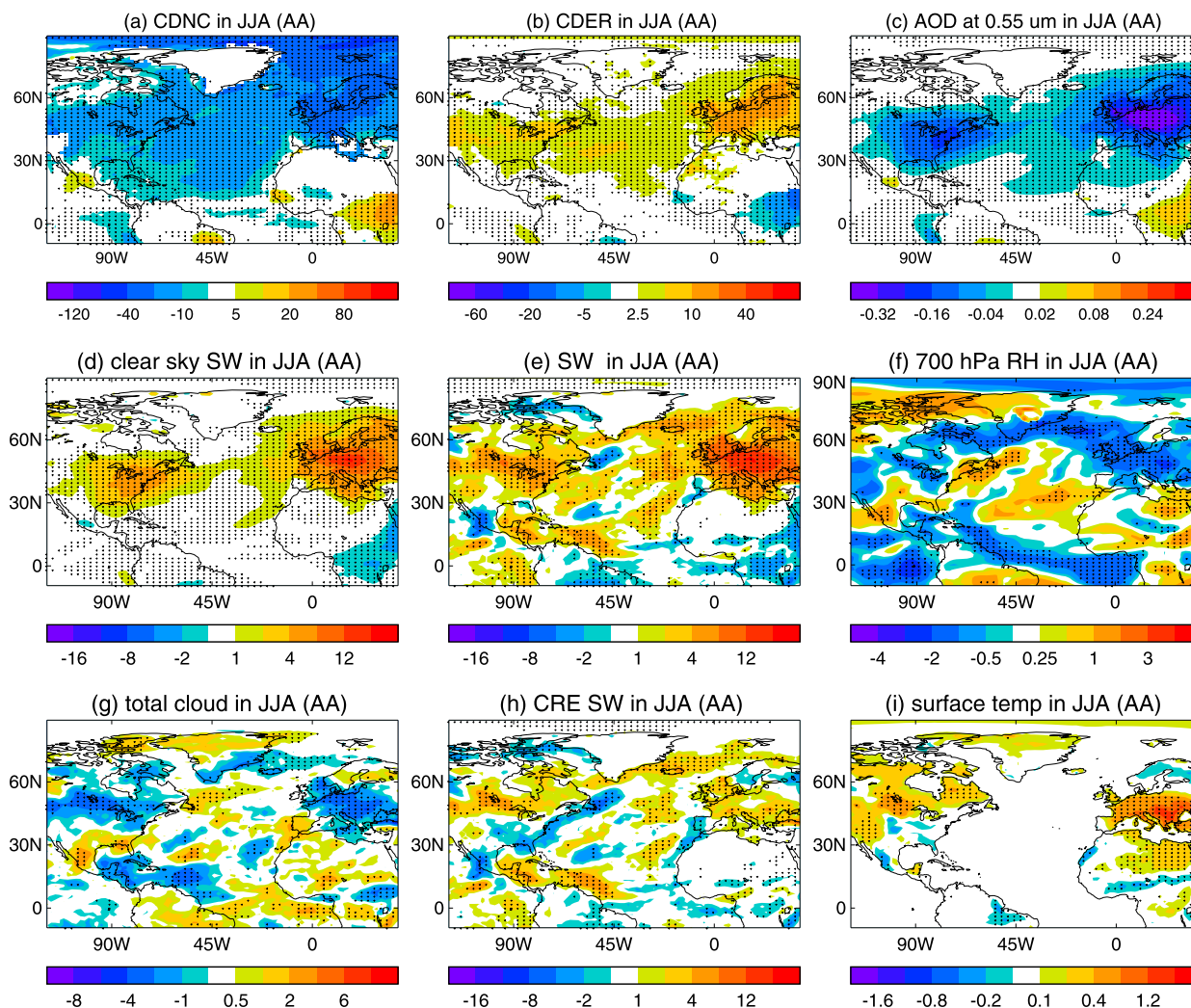


FIG. 6. Simulated climatological seasonal mean responses in JJA to AA emission changes ($SST_{AA} - SST$): (a) cloud droplet number concentration (CDNC), (b) cloud droplet effective radius (CDER), (c) AOD at $0.55 \mu\text{m}$, (d) surface clear-sky SW radiation, (e) surface SW radiation, (f) relative humidity at 700 hPa (%), (g) cloud fraction (%), (h) surface shortwave cloud radiative effect (CRE SW), and (i) surface temperature ($^{\circ}\text{C}$). Radiation is positive downward. Changes in CDNC and CDER are percentage changes relative to the experiment CON. Dots highlight regions where differences are statistically significant at 10% level based on the two-tailed Student's t test.

a weakening of the meridional temperature gradient in the troposphere around 45° – 55°N and a strengthening around 35° – 40°N (Fig. 7d). However, in contrast to the European sector the maximum anomalous temperature gradients are not found near the surface in this sector. This suggests a different mechanism is responsible for the circulation changes here. One possibility is a remote influence from the tropical Atlantic (possibly suggested by Fig. 5h), involving both barotropic and baroclinic components. Changes in clouds (Fig. 6g) and associated diabatic heating, which might be due to changes in absorbing aerosols (Shen and Ming 2018), could also play a more important role than changes in surface temperature gradients in this sector. Last, over the North Atlantic sector there is a significant response in midlatitudes (Fig. 7b), primarily in the

western Atlantic (Fig. 5h), which is dominated by the barotropic component (Figs. 7e,h,k,n).

2) RESPONSE TO CHANGES IN SST/SIE

In contrast to anthropogenic aerosol forcing, changes in SST/SIE not surprisingly have little effect on CDNC, CDER, and AOD (Fig. S6). However, the SST/SIE forcing does induce changes in clouds and hence shortwave (SW) radiation. In particular, a dipole pattern is induced with decreases in cloud amount (associated with increases in SW radiation) over the midlatitude Atlantic extending through central Europe, and increases in cloud amount (associated with decreases in SW radiation) in the subtropical Atlantic, extending over North Africa and the Mediterranean Sea. These changes in

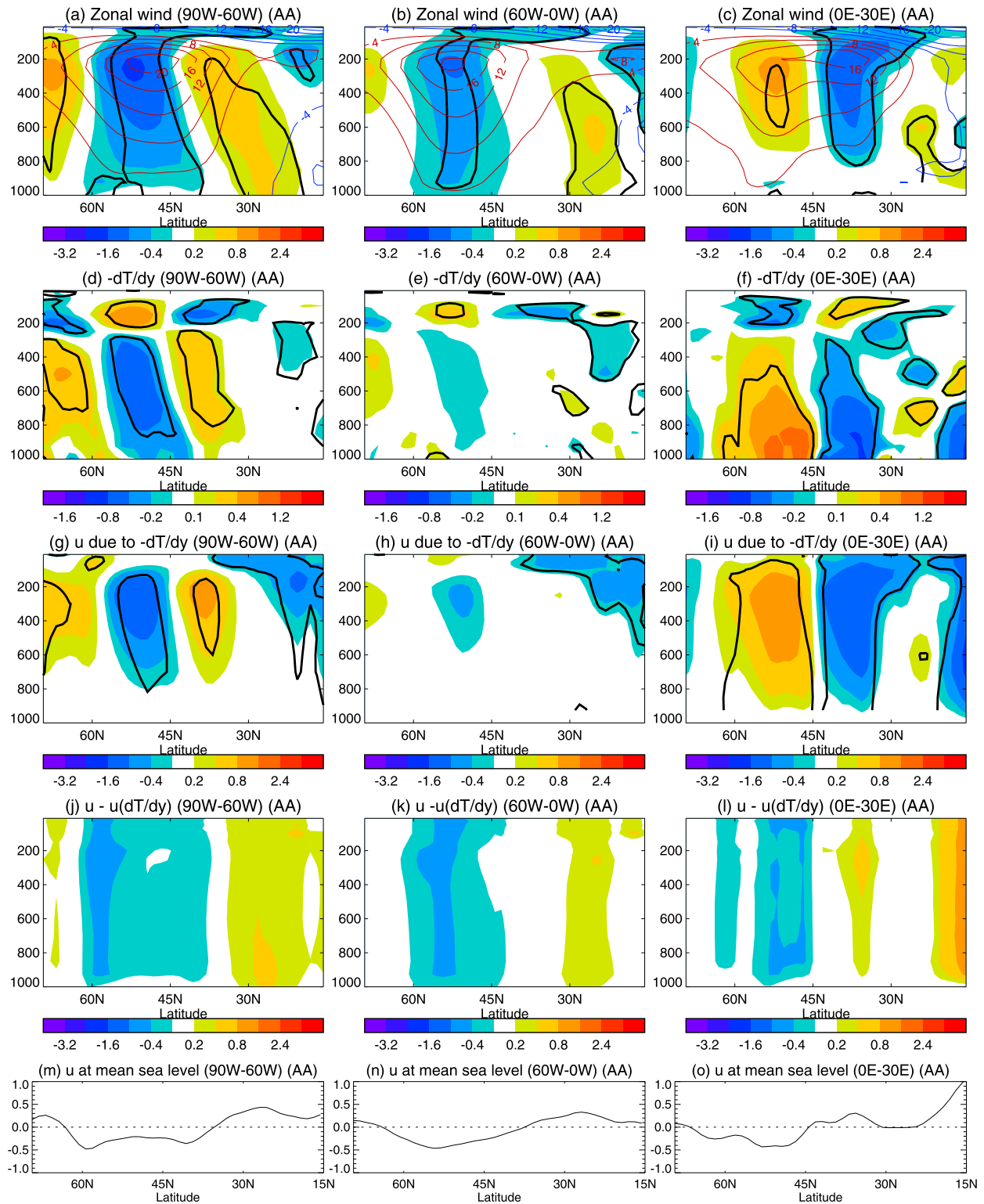


FIG. 7. Simulated (a)–(c) zonal wind changes (m s^{-1}), (d)–(f) meridional temperature gradient (K per 1000 km), (g)–(i) zonal wind changes from the thermal wind balance related to meridional temperature gradient, (j)–(l) zonal wind change residual, and (m)–(o) geostrophic zonal wind changes at mean sea level from SLP changes for the three sectors 90°–60°W, 60°–0°W, and 0°–30°E in response to changes in AA (SSTAA – SST). Thin red (westerly) and blue (easterly) lines (a)–(c) are the climatology of the CON simulation. Thick lines highlight regions where differences are statistically significant at 10% level based on the two-tailed Student's t test.

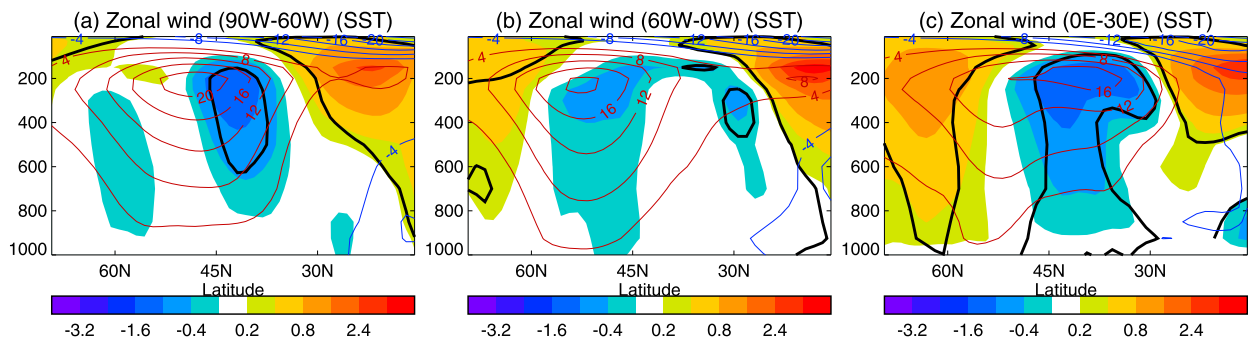


FIG. 8. Simulated (a)–(c) zonal wind changes (m s^{-1}) for the three sectors 90° – 60° W, 60° – 0° W, and 0° – 30° E in response to changes in SST/SIE (SST – CON). Thin red (westerly) and blue (easterly) lines in (a)–(c) are the climatology of the CON simulation. Thick lines highlight regions where differences are statistically significant at 10% level based on the two-tailed Student's t test.

clouds are consistent with changes in relative humidity and are likely to be linked to the changes in atmospheric circulation seen in Fig. 5k.

The changes in zonal winds in the three sectors in response to global SST/SIE changes are illustrated in Fig. 8. In all three sectors, in contrast to the AA response, there are anomalous westerlies in the upper troposphere around 15° – 30° N (Figs. 8a–c). This feature suggests that changes in the tropical circulation likely play an important role in the model's response to SST/SIE perturbations. The responses in midlatitudes show greater differences between the sectors. Over the North American sector, there are negative zonal wind anomalies, peaking in the upper troposphere, around 35° – 45° N to the south of the jet core (Fig. 8a). Over the North Atlantic, negative zonal wind anomalies are located close to the core of the jet around 45° – 55° N (Fig. 8b) and hence correspond to a weakening of the jet. Over western Europe (Fig. 8c), negative zonal wind anomalies are again located close to the core of the jet, here located around 35° – 45° N. The significant large anomalies are limited to the upper troposphere and correspond to a weakening of the Mediterranean jet. North of 60° N there are positive anomalies with a largely barotropic vertical structure.

The zonal wind responses to changes in SST/SIE in the Atlantic sector are similar to those in response to global SST/SIE changes over the North Atlantic sector and especially very similar over European sector, but show large differences over the North American sector (Figs. 9a–c). This clearly suggests that the latter region is strongly influenced by SST anomalies outside the Atlantic (e.g., Schubert et al. 2009; Seager et al. 2010) with a large baroclinic component (Figs. 9d,g,j,m) whereas the former responses are mainly influenced by Atlantic SST anomalies. We focus here on the Atlantic and European sector responses.

Over the North Atlantic sector, the weakening of the jet occurs in the latitude band around 50° N where the meridional SST gradient is weakened (Fig. 3c). A weakened temperature gradient is also seen in the lower troposphere in this latitude band (Fig. 9e). The zonal wind anomalies, involving both baroclinic and barotropic components (Figs. 9h,k,n), are consistent with a response of the eddy-driven jet to the anomalous SST gradient (e.g., Kushnir et al. 2002; Brayshaw et al. 2008;

Baker et al. 2017, 2019; Dunstone et al. 2019). However, there could also be a role for SST anomalies in the tropical Atlantic (Figs. 3c,f) exciting a remote response in the midlatitudes (e.g., Cassou et al. 2005; Sutton and Hodson 2007; Ghosh et al. 2017, 2019; Wulff et al. 2017; Osborne et al. 2020) and/or changes in Arctic sea ice (Petrie et al. 2015a,b; Coumou et al. 2018).

Over the western European sector, there is also likely to be a role for anomalous surface temperature gradients, as suggested by Fig. 9f. However, the strongest and most significant responses are seen in the upper troposphere, including in the tropics with a larger baroclinic component (Fig. 9i) than barotropic component (Figs. 9l,o). This suggests that the response in this sector may be strongly influenced by SST anomalies in the tropical Atlantic, consistent with Ghosh et al. (2019).

c. Precipitation changes over western Europe in response to different forcings

Associated with the changes in atmospheric circulation over the North Atlantic and western European sectors in response to different forcings are precipitation changes over Europe (Fig. 10). They generally show increased precipitation in northern Europe and decreased precipitation in southern Europe. The largest anomalies are seen in the SSTAA experiment, followed by the ALL experiment. Compared to the observations (Fig. 3e) the largest anomalies are located farther north and the positive anomalies are weaker than observed. These differences likely reflect the influence of biases in the model mean state (Fig. 4) and internal variability.

5. Discussion

The model experiments have shown a significant impact on the summer atmospheric circulation over the North Atlantic sector of decadal changes in both anthropogenic aerosol (AA) forcing and sea surface temperatures/sea ice extent (SST/SIE). In this section we discuss further the comparison between the results from our experiments and observed changes in atmospheric circulation, focusing on the European and Atlantic sectors.

In the model, circulation changes in the European sector—specifically a poleward shift and weakening of the

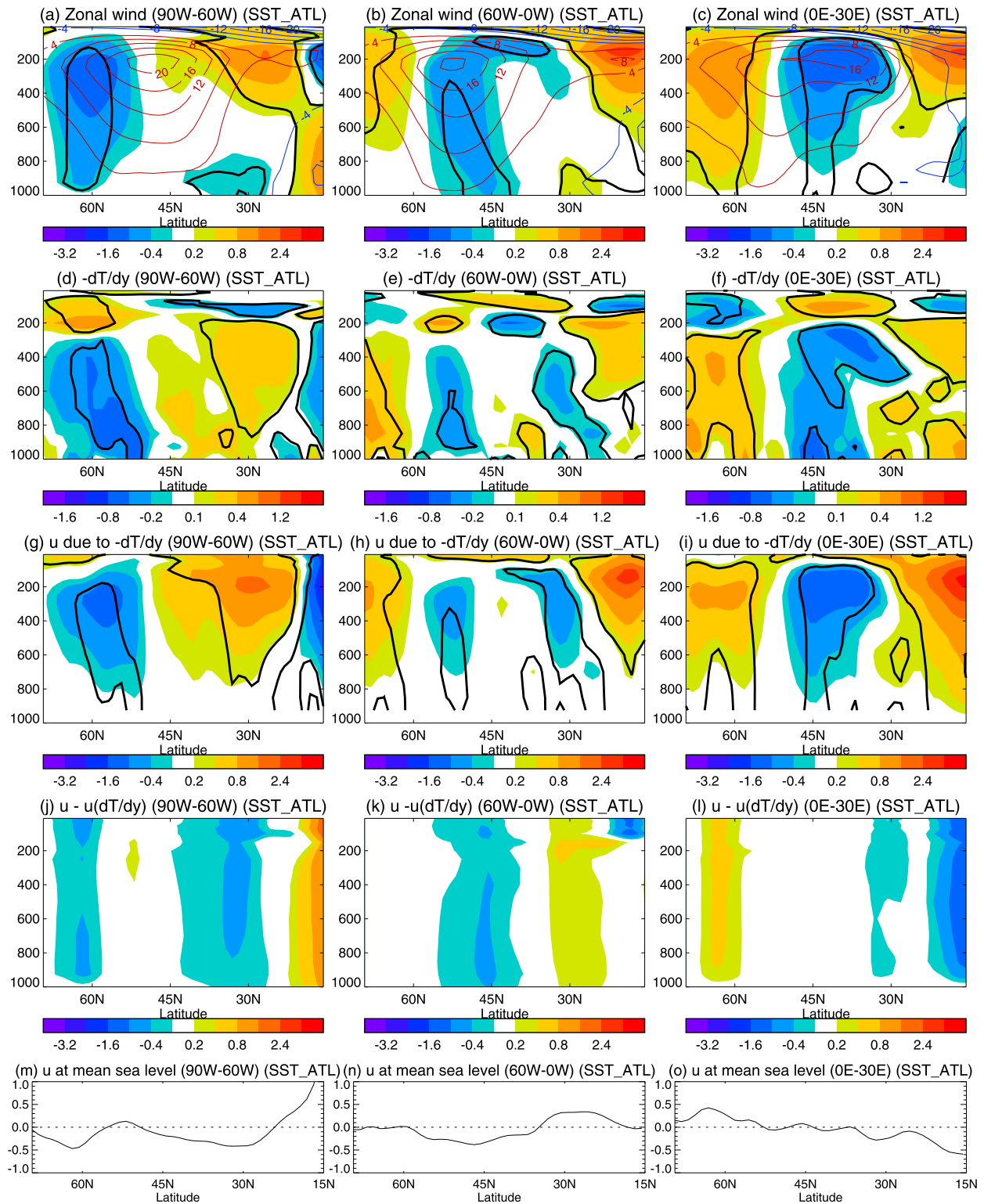


FIG. 9. Simulated (a)–(c) zonal wind changes (m s^{-1}), (d)–(f) meridional temperature gradient (K per 1000 km), (g)–(i) zonal wind changes from the thermal wind balance related to meridional temperature gradient, (j)–(l) zonal wind change residual, and (m)–(o) geostrophic zonal wind changes at mean sea level from SLP changes for the three sectors 90° – 60° W, 60° – 0° W, and 0° – 30° E in response to changes in SST/SIE over the Atlantic sector ($\text{SST} - \text{SST}_{\text{NoAtl}}$). Thin red (westerly) and blue (easterly) lines (a)–(c) are the climatology of the CON simulation. Thick lines highlight regions where differences are statistically significant at 10% level based on the two-tailed Student's t test.

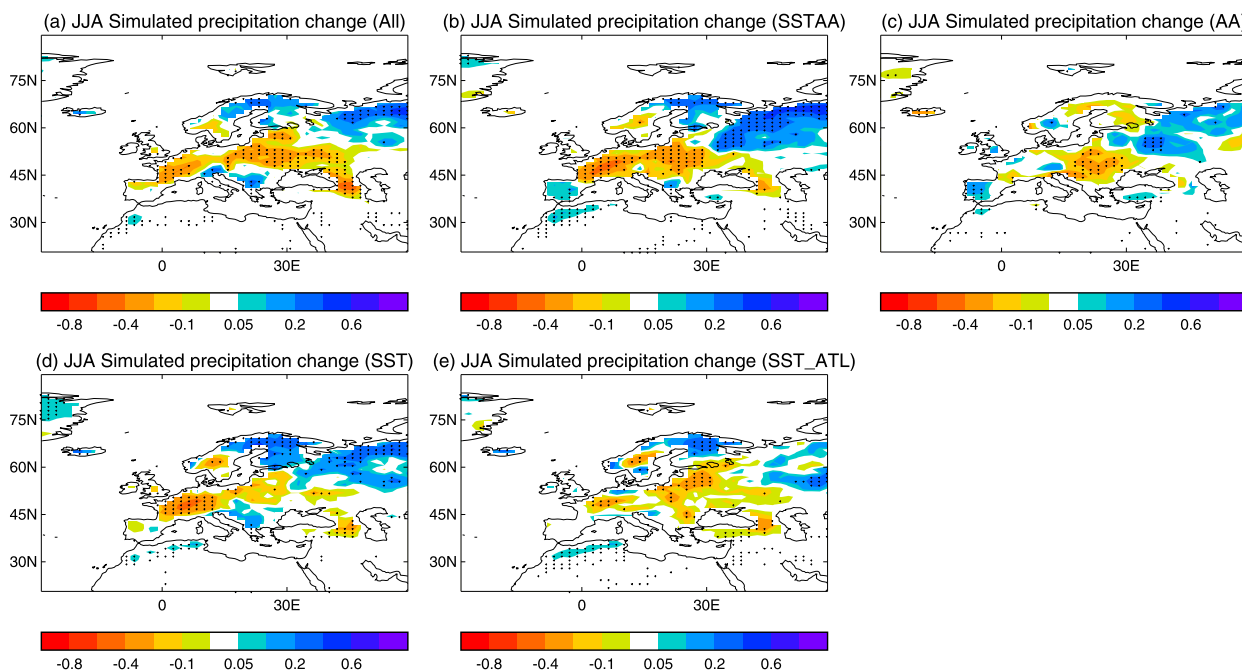


FIG. 10. Simulated climatological seasonal mean responses of precipitation (mm day^{-1}) to different forcings in JJA. Dots highlight regions where differences are statistically significant at 10% level based on the two-tailed Student's t test. (a) Responses to ALL forcings (ALL – CON) (b) responses to changes in SST/SIE and AA (SSTAA – CON), (c) response to changes in AA (SSTAA – SST), (d) responses to changes in SST/SIE (SST – CON), and (e) responses to changes in SST/SIE over the Atlantic sector (SST – SSTNoAtl).

Mediterranean jet—appear to be primarily a fast response to changes in AA, with a secondary role for changes in SST/SIE. This poleward shift and weakening of the Mediterranean jet show very good agreement with the observed changes in terms of vertical structure and magnitude. Both observations and the model simulated responses to combined changes in AA and SST/SIE (Fig. S7) show, in the upper troposphere (~ 200 hPa), increased westerlies of $1.5\text{--}2\text{ m s}^{-1}$ around 50°N and a decrease in the jet core speed of $2\text{--}2.5\text{ m s}^{-1}$ at $35^\circ\text{--}40^\circ\text{N}$. The similarity between the observed changes and the model responses to AA and SSTAA suggests that *fast responses to AA changes were likely the primary driver of these significant changes in the regional atmospheric circulation*. Undorf et al. (2018a) in an analysis of CMIP5 multimodel historical coupled simulations found evidence of a similar poleward shift in the Mediterranean jet forced by AA changes in the period 1975–2005 (their Fig. 5b), but they did not discuss the vertical structure or comparison with observations.

In contrast to the European sector, the changes in atmospheric circulation over the Atlantic sector are, in the model, influenced by changes in both SST/SIE and AA. In both cases, the model simulates a weakening of the Atlantic jet that contrasts with the equatorward shift seen in observations. What could explain this difference? One possibility is the lack of explicit air–sea coupling in our experiments (e.g., Petrie et al. 2015b; Ghosh et al. 2019). Another possibility is the impact of model biases. Previous research (Brayshaw et al. 2008; Baker et al. 2017) has shown that the response of the jet to anomalous SST gradients is sensitive to the location of the anomalous SST

gradient *relative to* the mean position of the jet. In particular Baker et al. (2017), using a dry idealized model with imposed SST patches, showed that an equatorward jet shift is most sensitive to warming in the middle and high latitudes on the poleward flank of the jet. We showed in section 3b that there is a significant mean bias in the Atlantic jet in our model: the jet core is too strong, and it is located several degrees too far poleward compared to observations. This means that the imposed SST anomalies (Fig. 3c) lie, to a greater extent, underneath the mean jet rather than on its poleward flank. We hypothesize that this difference could be an important factor in explaining why our model experiments show a weakening of the Atlantic jet rather than the observed equatorward shift.

Undorf et al. (2018a) in their analysis of CMIP5 coupled simulations found evidence of an equatorward shift of the Atlantic jet forced by AA changes in the period 1975–2005 (see again their Fig. 5b). In line with observations, the SST changes in these simulations show warming on the poleward flank of the mean jet (their Fig. 4b); however, not surprisingly (given the inclusion of AA forcing only) the overall pattern of SST changes in these simulations is very different to that which was observed. The SST changes in the real world will have been influenced by multiple factors, and separation of these influences is beyond the scope of this study. However, it is important to note that just because our experiments indicate that the fast response to AA changes on the Atlantic jet may have been small, this does not preclude the possibility that AA changes may have contributed to influencing the Atlantic jet through

their influence on SST changes (e.g., Booth et al. 2012; Undorf et al. 2018a,b; Watanabe and Tatebe 2019).

A further question is why the ALL experiment, in which all the historical forcing (not including natural forcing) factors were changed simultaneously, does not show the best agreement with observations. It is plausible that the impact of GHG forcing on atmospheric circulation in the North Atlantic/European region in our model response is also biased, and might be too strong compared to the impact of other forcing factors.

A point of concern is that aerosol forcing in this model might be overestimated (e.g., Boucher et al. 2013; Rotstayn et al. 2015). This might lead to a too-strong temperature and circulation response to the aerosol forcing changes. The response in surface clear-sky shortwave radiation to AA changes shows positive anomalies of $8\text{--}10\text{ W m}^{-2}$ over western Europe in our experiments (Fig. 6d). Sanchez-Lorenzo et al. (2015) reported surface downward solar radiation trends of 4.2 (with 95% confidence intervals of $1.0\text{--}7.3$) W m^{-2} per decade over Europe in summer during 1986–2012 based on the Global Energy Balance Archive (GEBA). Using station observations, Manara et al. (2016) reported trends of surface clear sky shortwave radiation of $5.1 (\pm 0.9)$ and $4.3 (\pm 1.2)$ W m^{-2} per decade over northern and southern Italy in summer during 1970–2013. The model-simulated clear-sky surface shortwave radiation changes in our study are within the uncertainty ranges of these observational estimations (when accounting for the fact that our two periods used to generate differences are about three decades apart) and therefore do not suggest that the response to AA changes is too strong in our model.

A final issue is the concern that the design of our experiments assumes that the responses to different forcing factors add linearly. This assumption is often made for thermodynamic responses, but it is certainly the case that dynamical responses have greater potential to exhibit nonlinear behavior. The surprisingly large differences between the responses to SSTAA and ALL might be evidence of such nonlinearity. We therefore see this as a very important area for future work.

6. Conclusions

In this study, the observed characteristics and potential drivers of recent decadal changes in summer atmospheric circulation over the North Atlantic/European sector have been investigated. A set of atmospheric general circulation model experiments was carried out to explore the relative roles of different forcing factors in contributing to the changes observed between 1964–81 and 1994–2011, and to elucidate the physical processes involved. The main findings are summarized as follows:

- Observations and reanalyses show a substantial *equatorward* migration of the summer North Atlantic ($60^{\circ}\text{--}0^{\circ}\text{W}$) eddy-driven jet from the 1970s to 2010s. This migration is associated with weakening jet speed at $\sim 60^{\circ}\text{N}$ and strengthening at $\sim 45^{\circ}\text{N}$. By contrast, the Mediterranean jet over Europe ($0^{\circ}\text{--}30^{\circ}\text{E}$) weakened and migrated *poleward*, with the biggest shift occurring in the late 1970s and early 1980s. These

changes in atmospheric circulation were associated with more cyclonic storms traveling across the United Kingdom into northern Europe, and fewer over the Mediterranean, leading to wet summers in northern Europe and dry summers in southern Europe.

- Comparison between the model results and the observed changes strongly suggests that *anthropogenic aerosol forcing, through fast atmospheric and land surface responses, was likely the primary driver of the observed changes in the Mediterranean jet*. Simulation diagnostics suggest that aerosol–radiation and aerosol–cloud interactions led to changes in surface shortwave radiation and land surface temperatures which forced the changes in the atmospheric circulation. Changes in SST/SIE play a secondary role in our experiments.
- The North Atlantic jet shows a response to changes in both SST/SIE and AA, with the most important SST/SIE influence arising from Atlantic SST/SIE. However, the simulated response is characterized by a weakening and broadening of the jet rather than the equatorward shift seen in observations. We argue that this difference could be explained by biases in the mean jet simulated in the model. Specifically, the summertime North Atlantic jet is located too far north in the model (i.e., the equatorward flank is too weak and the poleward flank too strong). A consequence is that AMV-related weakening of the midlatitude meridional SST gradient leads, in the model, to a reduction in jet speed, whereas in the real world the same changes in SST lead to an equatorward shift of the jet latitude (e.g., Brayshaw et al. 2008; Baker et al. 2017). The question of whether AA changes contributed to the observed changes in SST (Booth et al. 2012) is not addressed in our study.

Our findings are in line with a substantial body of evidence that multidecadal changes in North Atlantic sea surface temperatures are an important driver of changes in North Atlantic summertime atmospheric circulation and in European climate (e.g., Knight et al. 2006; Folland et al. 2009; Sutton and Hodson 2005, 2007, Sutton and Dong 2012; Ghosh et al. 2017, 2019). In addition, however, they suggest that changes in anthropogenic aerosols not only affected surface temperatures in Europe (e.g., Ruckstuhl et al. 2008; Nabat et al. 2014; Dong et al. 2017; Tian et al. 2020) but also had significant effects on atmospheric circulation. Specifically, we suggest that decreases in AA emissions since the 1970s caused a northward shift and weakening of the Mediterranean jet.

Our study demonstrates that different physical processes are likely to be responsible for changes in the summer atmospheric circulation in different sectors of the North Atlantic/European region. Therefore, assessments of future changes and their climate impacts may be better done by considering these sectors separately. In addition, there are several issues that merit future work.

First, in this study only one model has been used. In further research it will be important to test our findings using other atmospheric models, which exhibit different—ideally reduced—biases in the North Atlantic jet. It will also be important to investigate potential sensitivity to the representation of

anthropogenic aerosols and aerosol–cloud processes, as there is large intermodel diversity (e.g., Wilcox et al. 2015). Second, as discussed in the previous section, another important area for future work will be to investigate the potential role of nonlinearities in shaping the atmospheric circulation response to different forcing factors. Third, in this study we have examined only the fast response to anthropogenic aerosols involving the atmosphere and land surface, while slower responses mediated by aerosol induced SST/SIE changes have not been considered as part of the aerosol impacts. There is an obvious need to use coupled ocean–atmosphere models to understand these slow responses, as well as to assess how combined fast and slow responses shape low-frequency variability of the jet streams and climate in the North Atlantic/European region.

Acknowledgments. This work was supported by the Natural Environment Research Council (NERC) North Atlantic Climate System Integrated Study (ACSIS) project. B.D. and R.S. are supported by the U.K. National Centre for Atmospheric Science at the University of Reading. We thank Kevin Hodges for producing storm track diagnostics. We would also like to thank Editor Isla Ruth Simpson and three anonymous reviewers for their constructive comments and suggestions on the early version of this paper.

REFERENCES

- Allan, R., and T. Ansell, 2006: A new globally complete monthly historical gridded mean sea level pressure dataset (HadSLP2): 1850–2004. *J. Climate*, **19**, 5816–5842, <https://doi.org/10.1175/JCLI3937.1>.
- Baker, H. S., T. Woollings, and C. Mbengue, 2017: Eddy-driven jet sensitivity to diabatic heating in an idealized GCM. *J. Climate*, **30**, 6413–6431, <https://doi.org/10.1175/JCLI-D-16-0864.1>.
- , —, C. E. Forest, and M. R. Allen, 2019: The linear sensitivity of the North Atlantic Oscillation and eddy-driven jet to SSTs. *J. Climate*, **32**, 6491–6511, <https://doi.org/10.1175/JCLI-D-19-0038.1>.
- Baldi, M., G. Dalu, G. Maracchi, M. Pasqui, and F. Cesarone, 2006: Heat waves in the Mediterranean: A local feature or a larger-scale effect? *Int. J. Climatol.*, **26**, 1477–1487, <https://doi.org/10.1002/joc.1389>.
- Barnes, E. A., S. Solomon, and L. M. Polvani, 2016: Robust wind and precipitation responses to the Mount Pinatubo eruption, as simulated in the CMIP5 models. *J. Climate*, **29**, 4763–4778, <https://doi.org/10.1175/JCLI-D-15-0658.1>.
- Bellouin, N., J. Rae, A. Jones, C. Johnson, J. Haywood, and O. Boucher, 2011: Aerosol forcing in the Climate Model Intercomparison Project (CMIP5) simulations by HadGEM2-ES and the role of ammonium nitrate. *J. Geophys. Res.*, **116**, D20206, <https://doi.org/10.1029/2011JD016074>.
- Blackburn, M., J. Methven, and N. Roberts, 2008: Large-scale context for the UK floods in summer 2007. *Weather*, **63**, 280–288, <https://doi.org/10.1002/wea.322>.
- Boé, J., and L. Terray, 2014: Land–sea contrast, soil–atmosphere and cloud–temperature interactions: Interplays and roles in future summer European climate change. *Climate Dyn.*, **42**, 683–699, <https://doi.org/10.1007/s00382-013-1868-8>.
- Booth, B. B. B., N. J. Dunstone, P. R. Halloran, T. Andrews, and N. Bellouin, 2012: Aerosols implicated as a prime driver of twentieth-century North Atlantic climate variability. *Nature*, **484**, 228–232, <https://doi.org/10.1038/nature10946>.
- Boucher, O., D. Randall, P. Artaxo, C. Bretherton, G. Feingold, P. Forster, and X. Zhang, 2013: Clouds and aerosols. *Climate Change 2013: The Physical Science Basis*, T. F. Stocker et al., Eds., Cambridge University Press, 571–657.
- Brayshaw, D. J., B. Hoskins, and M. Blackburn, 2008: The storm-track response to idealized SST perturbations in an aquaplanet GCM. *J. Atmos. Sci.*, **65**, 2842–2860, <https://doi.org/10.1175/2008JAS2657.1>.
- Cassou, C., L. Terray, and A. S. Phillips, 2005: Tropical Atlantic influence on European heat waves. *J. Climate*, **18**, 2805–2811, <https://doi.org/10.1175/JCLI3506.1>.
- Chen, W., and B. Dong, 2019: Anthropogenic impacts on recent decadal change in temperature extremes over China: Relative roles of greenhouse gases and anthropogenic aerosols. *Climate Dyn.*, **52**, 3643–3660, <https://doi.org/10.1007/s00382-018-4342-9>.
- Coumou, D., G. Di Capua, S. Vavrus, L. Wang, and S. Wang, 2018: The influence of Arctic amplification on mid-latitude summer circulation. *Nat. Commun.*, **9**, 2959, <https://doi.org/10.1038/s41467-018-05256-8>.
- DallaSanta, K., E. P. Gerber, and M. Toohey, 2019: The circulation response to volcanic eruptions: The key roles of stratospheric warming and eddy interactions. *J. Climate*, **32**, 1101–1120, <https://doi.org/10.1175/JCLI-D-18-0099.1>.
- Deser, C., and A. Phillips, 2009: Atmospheric circulation trends, 1950–2000: The relative role of sea surface temperature forcing and direct atmospheric forcing. *J. Climate*, **22**, 396–413, <https://doi.org/10.1175/2008JCLI2453.1>.
- Dong, B., R. T. Sutton, and T. Woollings, 2013a: The extreme European summer 2012 (in “Explaining Extreme Events of 2012 from a Climate Perspective”). *Bull. Amer. Meteor. Soc.*, **94**, S28–S32, <https://doi.org/10.1175/BAMS-D-13-00085.1>.
- , —, —, and K. Hodges, 2013b: Variability of the North Atlantic summer storm track: Mechanisms and impacts on European climate. *Environ. Res. Lett.*, **8**, 034037, <https://doi.org/10.1088/1748-9326/8/3/034037>.
- , —, and L. Shaffrey, 2017: Understanding the rapid summer warming and changes in temperature extremes since the mid-1990s over western Europe. *Climate Dyn.*, **48**, 1537–1554, <https://doi.org/10.1007/s00382-016-3158-8>.
- Dunstone, N., D. Smith, S. Hardiman, R. Eade, M. Gordon, L. Hermanson, G. Kay, and A. Scaife, 2019: Skilful real-time seasonal forecasts of the dry northern European summer 2018. *Geophys. Res. Lett.*, **46**, 12 368–12 376, <https://doi.org/10.1029/2019GL084659>.
- Folland, C. K., J. Knight, H. W. Linderholm, D. Fereday, S. Ineson, and J. W. Hurrell, 2009: The summer North Atlantic Oscillation: Past, present, and future. *J. Climate*, **22**, 1082–1103, <https://doi.org/10.1175/2008JCLI2459.1>.
- Ghosh, R., W. A. Müller, J. Baehr, and J. Bader, 2017: Impact of observed North Atlantic multidecadal variations to European summer climate: A linear baroclinic response to surface heating. *Climate Dyn.*, **48**, 3547–3563, <https://doi.org/10.1007/s00382-016-3283-4>.
- , —, A. Eichhorn, J. Baehr, and J. Bader, 2019: Atmospheric pathway between Atlantic multidecadal variability and European summer temperature in the atmospheric general circulation model ECHAM6. *Climate Dyn.*, **53**, 209–224, <https://doi.org/10.1007/s00382-018-4578-4>.
- Grise, K. M., and L. M. Polvani, 2014: The response of midlatitude jets to increased CO₂: Distinguishing the roles of sea surface

- temperature and direct radiative forcing. *Geophys. Res. Lett.*, **41**, 6863–6871, <https://doi.org/10.1002/2014GL061638>.
- Hall, R., R. Erdélyi, E. Hanna, J. M. Jones, and A. A. Scaife, 2015: Drivers of North Atlantic polar front jet stream variability. *Int. J. Climatol.*, **35**, 1697–1720, <https://doi.org/10.1002/joc.4121>.
- , J. M. Jones, E. Hanna, A. A. Scaife, and R. Erdélyi, 2017: Drivers and potential predictability of summer time North Atlantic polar front jet variability. *Climate Dyn.*, **48**, 3869–3887, <https://doi.org/10.1007/s00382-016-3307-0>.
- Hanna, E., T. E. Cropper, P. D. Jones, A. A. Scaife, and R. Allan, 2015: Recent seasonal asymmetric changes in the NAO (a marked summer decline and increased winter variability) and associated changes in the AO and Greenland Blocking Index. *Int. J. Climatol.*, **35**, 2540–2554, <https://doi.org/10.1002/joc.4157>.
- , X. Fettweis, and R. J. Hall, 2018: Recent changes in summer Greenland blocking captured by none of the CMIP5 models. *Cryosphere*, **12**, 3287–3292, <https://doi.org/10.5194/tc-12-3287-2018>.
- Harris, I., P. D. Jones, T. J. Osborn, and D. H. Lister, 2014: Updated high-resolution grids of monthly climatic observations—The CRU TS3.10 dataset. *Int. J. Climatol.*, **34**, 623–642, <https://doi.org/10.1002/joc.3711>.
- Hodges, K. I., 1994: A general method for tracking analysis and its application to meteorological data. *Mon. Wea. Rev.*, **122**, 2573–2586, [https://doi.org/10.1175/1520-0493\(1994\)122<2573:AGMFTA>2.0.CO;2](https://doi.org/10.1175/1520-0493(1994)122<2573:AGMFTA>2.0.CO;2).
- Hurrell, J. W., Y. Kushnir, G. Ottersen, and M. Visbeck, 2003: *The North Atlantic Oscillation: Climate Significance and Environmental Impact*. *Geophys. Monogr.*, Vol. 134, Amer. Geophys. Union, 279 pp.
- Iles, C., and G. Hegerl, 2017: Role of the North Atlantic Oscillation in decadal temperature trends. *Environ. Res. Lett.*, **12**, 114010, <https://doi.org/10.1088/1748-9326/aa9152>.
- Iqbal, W., W. Leung, and A. Hannachi, 2018: Analysis of the variability of the North Atlantic eddy-driven jet stream in CMIP5. *Climate Dyn.*, **51**, 235–247, <https://doi.org/10.1007/s00382-017-3917-1>.
- Kalnay, E., and Coauthors, 1996: The NCEP/NCAR 40-Year Re-Analysis Project. *Bull. Amer. Meteor. Soc.*, **77**, 437–471, [https://doi.org/10.1175/1520-0477\(1996\)077<0437:TNYRP>2.0.CO;2](https://doi.org/10.1175/1520-0477(1996)077<0437:TNYRP>2.0.CO;2).
- Knight, J. R., C. K. Folland, and A. A. Scaife, 2006: Climate impacts of the Atlantic Multidecadal Oscillation. *Geophys. Res. Lett.*, **33**, L17706, <https://doi.org/10.1029/2006GL026242>.
- Kushnir, Y., W. A. Robinson, I. Bladé, N. M. J. Hall, S. Peng, and R. Sutton, 2002: Atmospheric GCM response to extratropical SST anomalies: Synthesis and evaluation. *J. Climate*, **15**, 2233–2256, [https://doi.org/10.1175/1520-0442\(2002\)015<2233:AGRTES>2.0.CO;2](https://doi.org/10.1175/1520-0442(2002)015<2233:AGRTES>2.0.CO;2).
- Lamarque, J. F., and Coauthors, 2010: Historical (1850–2000) gridded anthropogenic and biomass burning emissions of reactive gases and aerosols: Methodology and application. *Atmos. Chem. Phys.*, **10**, 7017–7039, <https://doi.org/10.5194/acp-10-7017-2010>.
- , and Coauthors, 2011: Global and regional evolution of short-lived radiatively-active gases and aerosols in the representative concentration pathways. *Climatic Change*, **109**, 191–212, <https://doi.org/10.1007/s10584-011-0155-0>.
- Livezey, R. E., and W. Y. Chen, 1983: Statistical field significance and its determination by Monte Carlo techniques. *Mon. Wea. Rev.*, **111**, 46–59, [https://doi.org/10.1175/1520-0493\(1983\)111<0046:SFSaid>2.0.CO;2](https://doi.org/10.1175/1520-0493(1983)111<0046:SFSaid>2.0.CO;2).
- Manara, V., M. Brunetti, A. Celozzi, M. Maugeri, A. Sanchez-Lorenzo, and M. Wild, 2016: Detection of dimming/brightening in Italy from homogenized all-sky and clear-sky surface solar radiation records and underlying causes (1959–2013). *Atmos. Chem. Phys.*, **16**, 11 145–11 161, <https://doi.org/10.5194/acp-16-11145-2016>.
- Nabat, P., S. Somot, M. Mallet, A. Sanchez-Lorenzo, and M. Wild, 2014: Contribution of anthropogenic sulfate aerosols to the changing Euro-Mediterranean climate since 1980. *Geophys. Res. Lett.*, **41**, 5605–5611, <https://doi.org/10.1002/2014GL060798>.
- O'Reilly, C. H., T. Woollings, and L. Zanna, 2017: The dynamical influence of the Atlantic multidecadal oscillation on continental climate. *J. Climate*, **30**, 7213–7230, <https://doi.org/10.1175/JCLI-D-16-0345.1>.
- Osborne, J. M., M. Collins, J. A. Screen, S. I. Thomson, and N. Dunstone, 2020: The North Atlantic as a driver of summer atmospheric circulation. *J. Climate*, **33**, 7335–7351, <https://doi.org/10.1175/JCLI-D-19-0423.1>.
- Ossó, A., R. Sutton, L. Shaffrey, and B. Dong, 2018: Observational evidence of European summer weather patterns predictable from spring. *Proc. Natl. Acad. Sci. USA*, **115**, 59–63, <https://doi.org/10.1073/pnas.1713146114>.
- Petrie, R. E., L. C. Shaffrey, and R. T. Sutton, 2015a: Atmospheric response in summer linked to recent Arctic sea ice loss. *Quart. J. Roy. Meteor. Soc.*, **141**, 2070–2076, <https://doi.org/10.1002/qj.2502>.
- , —, and —, 2015b: Atmospheric impact of Arctic sea ice loss in a coupled ocean–atmosphere simulation. *J. Climate*, **28**, 9606–9622, <https://doi.org/10.1175/JCLI-D-15-0316.1>.
- Rayner, N. A., and Coauthors, 2003: Global analyses of SST, sea ice and night marine air temperature since the late nineteenth century. *J. Geophys. Res.*, **108**, 4407, <https://doi.org/10.1029/2002JD002670>.
- Robson, J., and Coauthors, 2018: Recent multivariate changes in the North Atlantic climate system, with a focus on 2005–2016. *Int. J. Climatol.*, **38**, 5050–5076, <https://doi.org/10.1002/joc.5815>.
- Rotstain, L. D., M. A. Collier, S. J. Jeffrey, J. Kidston, J. I. Syktus, and K. K. Wong, 2013: Anthropogenic effects on the subtropical jet in the Southern Hemisphere: Aerosols versus long-lived greenhouse gases. *Environ. Res. Lett.*, **8**, 014030, <https://doi.org/10.1088/1748-9326/8/1/014030>.
- , —, D. T. Shindell, and O. Boucher, 2015: Why does aerosol forcing control historical global-mean surface temperature change in CMIP5 models? *J. Climate*, **28**, 6608–6625, <https://doi.org/10.1175/JCLI-D-14-00712.1>.
- Ruckstuhl, C., and Coauthors, 2008: Aerosol and cloud effects on solar brightening and the recent rapid warming. *Geophys. Res. Lett.*, **35**, L12708, <https://doi.org/10.1029/2008GL034228>.
- Sanchez-Lorenzo, A., M. Wild, M. Brunetti, J. A. Guijarro, M. Z. Hakuba, J. Calbó, S. Mystakidis, and B. Bartok, 2015: Reassessment and update of long-term trends in downward surface shortwave radiation over Europe (1939–2012). *J. Geophys. Res.*, **120**, 9555–9569, <https://doi.org/10.1002/2015JD023321>.
- Scherrer, S. C., M. Croci-Maspoli, C. Schwierz, and C. Appenzeller, 2006: Two-dimensional indices of atmospheric blocking and their statistical relationship with winter climate patterns in the Euro-Atlantic region. *Int. J. Climatol.*, **26**, 233–249, <https://doi.org/10.1002/joc.1250>.
- Schubert, S., and Coauthors, 2009: A U.S. CLIVAR project to assess and compare the responses of global climate models to

- drought-related SST forcing patterns: Overview and results. *J. Climate*, **22**, 5251–5272, <https://doi.org/10.1175/2009JCLI3060.1>.
- Seager, R., N. Naik, M. Ting, M. Cane, N. Harnik, and Y. Kushnir, 2010: Adjustment of the atmospheric circulation to tropical Pacific SST anomalies: Variability of transient eddy propagation in the Pacific–North America sector. *Quart. J. Roy. Meteor. Soc.*, **136**, 277–296, <https://doi.org/10.1002/qj.588>.
- Shen, Z., and Y. Ming, 2018: The influence of aerosol absorption on the extratropical circulation. *J. Climate*, **31**, 5961–5975, <https://doi.org/10.1175/JCLI-D-17-0839.1>.
- Shepherd, T. G., 2019: Storyline approach to the construction of regional climate change information. *Proc. Roy. Soc.*, **475A**, 20190013, <https://doi.org/10.1098/rspa.2019.0013>.
- Simpson, I. R., C. Deser, K. A. McKinnon, and E. A. Barnes, 2018: Modeled and observed multidecadal variability in the North Atlantic jet stream and its connection to sea surface temperatures. *J. Climate*, **31**, 8313–8338, <https://doi.org/10.1175/JCLI-D-18-0168.1>.
- Sutton, R., and D. Hodson, 2005: Atlantic Ocean forcing of North American and European summer climate. *Science*, **309**, 115–118, <https://doi.org/10.1126/science.1109496>.
- , and —, 2007: Climate response to a multidecadal warming and cooling of the North Atlantic Ocean. *J. Climate*, **20**, 891–907, <https://doi.org/10.1175/JCLI4038.1>.
- , and B. Dong, 2012: Atlantic Ocean influence on a shift in European climate in the 1990s. *Nat. Geosci.*, **5**, 788–792, <https://doi.org/10.1038/ngeo1595>.
- Tian, F., B. Dong, J. Robson, R. Sutton, and L. Wilcox, 2020: Processes shaping the spatial pattern and seasonality of the surface air temperature response to anthropogenic forcing. *Climate Dyn.*, **54**, 3959–3975, <https://doi.org/10.1007/s00382-020-05211-8>.
- Tibaldi, S., and F. Molteni, 1990: On the operational predictability of blocking. *Tellus*, **42**, 343–365, <https://doi.org/10.3402/tellusa.v42i3.11882>.
- Undorf, S., M. A. Bollasina, and G. C. Hegerl, 2018a: Impacts of the 1900–74 increase in anthropogenic aerosol emissions from North America and Europe on Northern Hemisphere summer climate. *J. Climate*, **31**, 8381–8399, <https://doi.org/10.1175/JCLI-D-17-0850.1>.
- , —, B. B. B. Booth, and G. C. Hegerl, 2018b: Contrasting the effects of the 1850–1975 increase in sulphate aerosols from North America and Europe on the Atlantic in the CESM. *Geophys. Res. Lett.*, **45**, 11 930–11 940, <https://doi.org/10.1029/2018GL079970>.
- Walters, D. N., and Coauthors, 2017: The Met Office Unified Model Global Atmosphere 6.0/6.1 and JULES Global Land 6.0/6.1 configurations. *Geosci. Model Dev.*, **10**, 1487–1520, <https://doi.org/10.5194/gmd-10-1487-2017>.
- Watanabe, M., and H. Tatebe, 2019: Reconciling roles of sulphate aerosol forcing and internal variability in Atlantic multidecadal climate changes. *Climate Dyn.*, **53**, 4651–4665, <https://doi.org/10.1007/s00382-019-04811-3>.
- Wilcox, L. J., E. J. Highwood, B. B. B. Booth, and K. S. Carslaw, 2015: Quantifying sources of inter-model diversity in the cloud albedo effect. *Geophys. Res. Lett.*, **42**, 1568–1575, <https://doi.org/10.1002/2015GL063301>.
- Woollings, T., C. Czuchnicki, and C. Franzke, 2014: Twentieth century North Atlantic jet variability. *Quart. J. Roy. Meteor. Soc.*, **140**, 783–791, <https://doi.org/10.1002/qj.2197>.
- Wulff, C. O., R. J. Greatbatch, D. I. V. Domeisen, G. Gollan, and F. Hansen, 2017: Tropical forcing of the summer east Atlantic pattern. *Geophys. Res. Lett.*, **44**, 11 166–11 173, <https://doi.org/10.1002/2017GL075493>.